Active Distribution System Resilience Quantification and Enhancement through Multi-microgrid and Mobile Energy Storage

[1*]Dillip Kumar Mishra, [1]Mojtaba Jabbari Ghadi, [1]Li Li, [2]Jiangfeng Zhang, [1]M. J. Hossain

[1]School of Electrical and Data Engineering, University of Technology, Sydney, NSW 2007, Australia

[3]Department of Automotive Engineering, Clemson University, Greenville, SC 29607, United States

Corresponding author: *dkmishra@ieee.org

Abstract: The functional capability of the active distribution network is continually challenged by extreme weather and unforeseen events. A complete resilience quantification framework is required to assess the resilience of a distribution system. With this objective, a framework for demonstrating resilience enhancement through the utilization of multi-microgrids (MMGs) and mobile energy storage in extreme operating conditions is developed in this paper. In the proposed framework, four resilience indices, that is, withstand, recovery, adapt, and prevent (WRAP), are introduced. Withstand index signifies the coping capability after the event, where the MG plays a vital role. The recovery index measures the restoration after the event ends through the system reconfiguration using MGs, tie-lines, and mobile energy storage. The adapt index shows the stability of the system before and during the events. Finally, the prevent index suggests how different resources are important and responsible for fast recovery and minimizing consequences. WRAP, as a resilience quantification framework, is formulated in this study, and indices are quantified and enhanced through the MMG and mobile energy storages. The IEEE 33-bus system is considered for this study, and simulation is performed with different scenarios and measured resilience indices. It is found that appropriate reconfiguration through the use of MMG, tie-lines, and mobile storages can remarkably enhance the resilience of a distribution system.

Keywords: Active distribution system, Mobile energy storage, Multimicrogrid, Resilience

NOMENCLATURE

Acronyms

ADS	Active distribution system
DG	Diesel generator
BES	Battery energy storage
CL	Critical load
DER	Distributed energy resource
MG	Microgrid
MMG	Multi-microgrid
MSU	Mobile storage unit
SCC	Short circuit capacity
SOC	State of charge
TL	Tie-line

VSI	Voltage stability index
WRAP	Withstand- Recover- Adapt- Prevent

Sets and Indices

D,d	Set and index of DG units
R,r	Set and index of renewable generation units
B,b	Set and index of energy storage units
H,h	Set and index of MSU units
L,l	Set and index of loads
T,t	Set and index of time instants

Parameters and variables

M	Number of loads picked up by DERs for each scenario
N	Number of disaster scenarios considered
C_b	Operation cost of battery b
C_d	Unit generation cost of DG d
C_h	Transportation cost of MSU m per kM
C_l	Load shedding cost of load l
C_r	Unit generation cost of renewable generation unit r
D_h	Distance traveled by MSU h in kMs
E_b^{min}, E_b^{max}	Minimum/maximum energy stored in battery b
$E_{b,t}$	Battery SOC at time instant t
P_b	Active power generation by battery b
P_d	Active power generation by DG d
P_d^{min}/P_d^{max}	Minimum/maximum active power by DG d
P_l	Load curtailment at load point l after the event
$P_{LD,l}$	Total load demand at load point l
P_r	Active power generation by PV
$P_{CL,k}^j$	Critical load of k^{th} load point restored after j^{th} extreme event
$P_{b,t}^{ch}(P_{b,t}^{ch,max})$ $/P_{b,t}^{dis}(P_{b,t}^{dis,max})$	Charging/discharging power (limit)
R_U , R_D	Ramp-up/down rates of DG units
$\mathfrak{R}_{\mathrm{W}}$ and $\mathfrak{R}_{\mathrm{R}}$	Withstand and Recover index, respectively
$\mathfrak{R}_{\mathrm{A}}$ and $\mathfrak{R}_{\mathrm{P}}$	Adapt and Prevent index, respectively
t_{rsT} / t_{reT}	Restoration start/end time for traditional system
Δt	Timeslot duration
$\delta_{b,t}^{i,ch}$ / $\delta_{b,t}^{i,dis}$	Charge/discharge binary indicators of BESs
$\eta_{b,t}^{i,ch}$ / $\eta_{b,t}^{i,dis}$	Charging/discharging efficiency
t_{ds} / t_{de}	Disturbance start/end time
t_{rs} / t_{re}	Restoration start/end time

1. Introduction

Current power distribution systems experience frequent power outages across the globe due to increasing natural disasters and cyber attacks. In addition, the power systems are designed following reliability principles, i.e., security and adequacy [1]. With these principles, the power system can only cope with high-probability and low-impact events, mostly the known failures, where it is unremarkably affected and can be restored within a reasonable time with lesser impacts on energy end-users. However, in the past few decades, catastrophic events increased, significantly impacting end-users, and the reliability-based design can not ensure stable operation [2]. The evidence includes major catastrophic events, such as Hurricane Sandy and Katrina, Japan earthquake, Ukraine

cyber-physical attack, and other major events reported in [3-5]. These events affected millions of people and caused energy infrastructure damages, significantly impacting lives and the economy. Thus, to ensure a reduced impact on the economy against the power system damage and energy security, the distribution system should be resilient in dealing with four major attributes, withstand, recover, adapt, and prevent (WRAP).

In the context of the power system, resilience deals with high-impact and low-probability (HILP) events. Hence, to minimize the consequence against HILP events, power system decentralization is necessary, particularly in the distribution system. In order to obtain the decentralized system, the microgrid (MG) and smart grid technology are vital, where the integration of distributed energy resources (DERs) play a key role. Subsequently, the interconnection of microgrids termed as multi-MG (MMG) is further pursued as a resilient-based design [6]. With the help of such technology, the distribution system is termed as an active distribution system (ADS). In addition, optimal reconfiguration and mobile services are significant for the fast load recovery and resilience enhancement of the ADS.

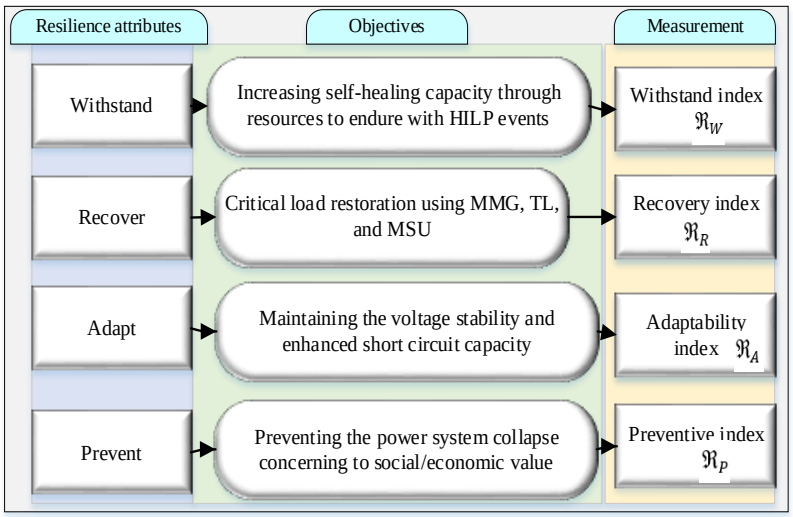

Fig. 1. WRAP framework and measurement indices

In recent decades, several studies have been conducted to improve the power system resilience, including the ADS. On the other hand, various resilience indices have been proposed to quantify the system performance. As noted, the WRAP factors are extremely important for resilience studies. The detailed discussion is provided in Section III, where the authors have explained each factor and its relevance. Moreover, each factor of WRAP has significant value, and to enhance it, several methods have been used [6-16]. In [6, 7], the importance of renewable energy penetrations in ADS is discussed in terms of MG and MMG technology. The main aim is to increase the self-healing capability that refers to the withstand of a system. The authors in [8-10] address the restoration techniques and their enhancement strategies through optimal reconfiguration of resources such as tie-lines and mobility services (mobile energy storage and crew member [11, 12]). From the past few years, an intensive research has been carried out to enhance the resiliency of the ADS through mobile power sources such as EV fleets, truck-mounted mobile energy storage systems, and mobile energy emergency generators [8, 9, 17, 18]. In addition, the viability of mobile power sources for distribution system restoration in terms of cost-effectiveness and scheduling is discussed in [19]. Further, to enhance the adaptability of a system, a graph theory approach is developed using algebraic connectivity and betweenness centrality in [13, 14]. Finally, preventive planning is a

major concern, which can reduce the future power outage by assessing the past experience through probability measures as discussed in [15, 16]. All four factors are combined in this study to introduce a resilience quantification framework, WRAP.

Notably, various resilience quantification frameworks have been developed, such as RRRA (resourcefulness, recovery, robustness, and adaptability) by Abbasi et al. [13], where the authors have proposed 4 indices and considered only the black start unit using a large battery to restore the load. However, sometimes the disaster magnitude is very high, and a number of lines can be disconnected; thus, the same operation might be affected. Considering the above issue, we have presented the resilience quantification framework as well as the enhancement technique through reconfiguration and mobile storage units in the wake of single and multi-fault analysis. In Ref. [20], Panteil et al. developed FLEP (fast, low, extensive, promptly), and this paper has focused on transmission networks using fragility modelling. According to the tower condition, the FLEP can be measrured. In [14], Srivastava et al., have developed the resilience indices through the graph theory approach, and the enhancement of resilience is ensured by switching operation. But, in our case, the resilience enhancement is achieved by using reconfiguration and mobile storage units. Apart from the above indices, a few others studies has been carried out to quantify the resilience indices such as degradation, restoration efficiency, and MG resilience index [21], resilience achievement worth [22], expected energy curtailment [23], grid recovery index [24], sub resilience index[25], grid resilience metric [26], severity risk index [27], and a few more are reported in [28, 29]. Due to increasedcyber-attacks from the last few decades [30], authors in [31, 32] presented the cyber-physical power system to monitor the microgrid resiliency. However, those indices do not reflect the whole process of the event (pre, during, and post). Although a few studies have contributed to the resilience indices, all do not have the same test case and scenarios, e.g., studies are considered on high wind storm, ice storm, cyber-attacks, single line or multi-line failure, and on the other hand, either the indices are considered for transmission or distribution systems. However, our model is for expansion planning and operation in an active distribution systemusing reconfiguration and mobility services to enhance the system resilience. In addition, we have applied the multi-fault scenarios where the grid outage is taken into consideration, and then the critical load has been restored through the multi-microgrid and mobility service approach. In a nutshell, this paper has a significant value in terms of resilience quantification framework, enhancement techniques, and load recovery in an expansion planning and operation stage while considering the grid-connected and grid outage conditions.

The main contributions of this study are as follows.

- A two-stage programming model is proposed to improve the resilience of an ADS. In stage I, a normal operational scheme is implemented to minimize operating costs. In stage II, an unforeseen event is applied, and the critical loads are restored to normal operation, where the critical load maximization is considered as an objective function.
- Furthermore, the resilience quantification framework, WRAP, is developed to measure the system's resiliency.
- The proposed strategy considers the optimal allocation of MGs and TLs to minimize the load curtailment. In addition, MSUs are allocated optimally as an emergency source to enhance the system's resiliency.

- This proposed approach provides a complete solution for expansion planning and operational scheme through the WRAP framework, where all four attributes, withstand, recover, adapt, and prevent stages, are well defined and measured to show the resiliency of the ADS.
- The prominent feature of the proposed WRAP framework is tested through the IEEE 33-bus test system with different scenarios.

The remainder of the paper is organized as follows. Section II defines the resilience quantification framework. System modeling that includes objective function, constraints, and resilience index is presented in Section III. Thereafter, the results are reported in Section IV, followed by the conclusion and further recommendation in Section V.

2. Proposed Resilience Quantification Framework

As noted earlier, the WRAP framework, where four significant factors are used to show the resiliency of the ADS in terms of coping capacity after the HILP event, rapid recovery through available resources, measurestability during and after the event, and preventive measurement. The short description of the WRAP framework with its objective and proposed index is presented in Fig. 1. The four major attributes to resilience are shown in Fig. 2, representing how the resources are responsible for the system performance level. The detailed discussions of the characteristics of the WRAP framework are as follows. Fig. 2 shows the system performance according to the event period, such as pre, during, and post. The pre-event is the normal operation, i.e., before t_{ds}; from t_{ds} to t_{de} is the during-event; from t_{de} to t_{re} is the post-event, and then comes the normal operation. From t_{ds} to t_{re}, the system operator should consider the four main factors concerning the system's resilience within the event period. Moreover, these factors can show the resiliency of the system by utilizing a number of resources. For instance, the contribution of MGs can enhance the system resiliency and serve more loads after the event, which is considered as withstand phase.

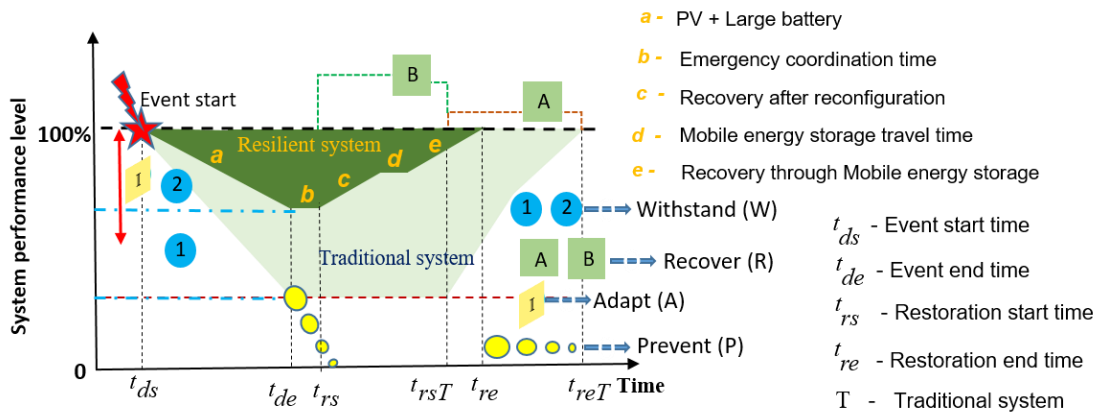

Fig. 2. System performance curve with four major attributes to resilience

The fault occurs at t_{ds} and can continue for a few minutes or hours. During that time, if the system does not have any other resources except grid supply, it might fail to supply all the CLs, thereby resulting in system collapse. However, if the resources, such as MGs, are available, they can supply the CLs which are connected inside the MG. On the contrary, the CLs, which are outside the MG, cannot be supplied if the grid fails. Moreover, the system can withstand some of the CLs during the events to minimize the impact of an event, represented as 1

and 2 (in the blue circle) in Fig. 2. After t_{de}, the restoration process begins. However, switching the topology or DERs into operation requires considerable time. Thus, it can be started from t_{rs} and end up to t_{re}. Moreover, the restoration can be performed when alternative resources or paths are sufficient because the original path may not have the grid supply to satisfy the load if the fault occurs on the lines. Thus, during that period, the DERs with TLs can satisfy the load demand either partially or fully. With this objective, less restoration time is required than usual, as shown in Fig. 2 (A and B in the green square). Here, 'A' considers the traditional system, which requires a longer time to restore the loads. Moreover, the recovery considering DERs is divided into three phases, namely, *c*, *d*, and *e*. During the c-phase, the restoration is conducted through the reconfiguration technique. However, sometimes, due to multiple events, it cannot restore all the CLs. Thus, MSUs are added, and they require a few minutes to reach the load center, presented as d-phase. Then, the remaining CLs can be recovered through MSUs, presented as e-phase.

Furthermore, as far as adaptability is concerned, sufficient resources, including DERs, storage, and alternative paths, such as TLs, can increase the system flexibility. This finding implies that the system can quickly switch from one point to another towards load recovery, indicating that the system could follow better resilient characteristics, presented as I (in the yellow parallelogram) in Fig. 2. Finally, the system operator should always consider assessing the impact after the event; it helps to minimize the total system collapse in the forthcoming event, which is the prevent phase. To prevent future events, the system should be hardened, and a decentralized network should be designed, as well as a better prediction strategy. In addition, to reduce the outage duration, the recovery time should be fast. This condition can be obtained by system reconfiguration using TLs and DERs, as well as the adaptive formation of MGs and mobile services, such as MSUs, mobile substation, crews, and mobile de-icing devices. The system can be robust, and eventually, the power loss and outages can be reduced by considering this design. A detailed discussion of the introduced WRAP indices is presented in the following section

3. Resilient System Formulation

3.1. Objective function

This section deals with the problem formulation, such as objective functions, system constraints, and resilience indices. The objective is to minimize operational cost and maximize critical load restoration while satisfying operational constraints and ensuring radial operation. Eqs. (1) and (2) present the objective function of minimizing the operational cost and maximizing the critical load pickup, respectively.

$$\min_{t \in T} \left| \left(\sum_{r \in R} C_r P_{r,t} \right) + \left(\sum_{d \in D} C_d P_{d,t} \right) + \left(\sum_{b \in B} C_b P_{b,t} \right) + \left(\sum_{l \in L} C_l P_{l,t} \right) + \left(\sum_{h \in H} C_h D_{h,t} \right) \right| \quad (1)$$

$$max \sum_{j=1}^{N} \sum_{k=1}^{M_j} P_{CL,k}^{j} \quad (2)$$

3.2. System Constraints

For each MG *i* and at each timeslot *t*, the sum of the total generated power by DER and DG units, charging/discharging power of BESs, and curtailed load must be equal to the total load, expressed in (3). The ramping up and down of the DG unit limits is expressed in (4), (5), and (6). The curtailment of load demand must

not exceed the total load, as expressed in (7). In storage unit constraints, the permissible charging/discharging limits of power are expressed in (8) and (9) with energy limits in (10). Simultaneous charging and discharging of the storage unit should be avoided; the constraint can be written as (11). Eq. (12) represents the relationship between the energy and charging/discharging power.

$$\sum_{r \in R_i} P_{r,t}^{i} + \sum_{d \in D_i} P_{d,t}^{i} + \sum_{b \in B_i} (P_{b,t}^{i,dis} - P_{b,t}^{i,ch}) = \sum_{l \in L_i} (P_{LD,l,t}^{i} - P_{l,t}^{i}) \qquad \forall i, t. \tag{3}$$

$$P_d^{min} \leq P_{d,t}^{i} \leq P_d^{max} \qquad \forall d, t, i \tag{4}$$

$$P_{d,t}^{i} - P_{d,t-1}^{i} \leq R_{U,d} \qquad \forall d, t, i \tag{5}$$

$$P_{d,t-1}^{i} - P_{d,t}^{i} \leq R_{D,d} \qquad \forall d, t, i \tag{6}$$

$$0 \leq P_{l,t}^{i} \leq P_{LD,l,t}^{i} \qquad \forall t, i \tag{7}$$

$$0 \leq P_{b,t}^{i,ch} \leq \delta_{b,t}^{i,ch} P_{b,t}^{ch,max}, \delta_{b,t}^{i,ch} \in \{0,1\} \qquad \forall b, t, i \tag{8}$$

$$0 \leq P_{b,t}^{i,dis} \leq \delta_{b,t}^{i,dis} P_{b,t}^{dis,max}, \delta_{b,t}^{i,dis} \in \{0,1\} \qquad \forall b, t, i \tag{9}$$

$$E_b^{min} \leq E_{b,t}^{i} \leq E_b^{max} \qquad \forall b, t, i \tag{10}$$

$$\delta_{b,t}^{i,ch} + \delta_{b,t}^{i,dis} = 1 \qquad \forall b, t, i \tag{11}$$

$$E_{b,t+1}^{i} = E_{b,t}^{i} + \left(P_{b,t}^{i,ch} \eta_{b,t}^{ch} \Delta t - P_{b,t}^{i,dis} \Delta t \Big/ \eta_{b,t}^{dis} \right) \qquad \forall b, t, i \tag{12}$$

3.3. Resilience Index

The performance of the ADS is evaluated by the proposed resilience quantification framework, WRAP.

3.3.1. Withstand

Withstand refers to the coping capacity of the system after the event. It indicates whether the system is completely collapsed or partially collapsed. The system can be a total outage when the grid supply is unavailable, and no additional generation unit is available in the system. However, the system with DERs can cope with extreme events and minimize outages. The withstand index ($\mathfrak{R}_W$) can be measured by (13) as follows:

$$\mathfrak{R}_{W,i} = \left(P_{CL,i} - P_{CL,0}\right) \times \left(t_{de} - t_{ds}\right) \tag{13}$$

where, $P_{CL,i}$ = Critical power available after considering MG i in kW, $P_{CL,0}$ = Critical active power available at the end of the event as a reference in kW.

3.3.2. Recover

The recovery index ($\mathfrak{R}_R$) measures the restored energy after the event, as expressed in (14). Different resources are used to restore the critical load in the recovery process, such as PV, BES, TL, and DG. In addition, if it still fails to recover all the CL, MSUs can be used.

$$\mathfrak{R}_{R,j} = \left(P_{CL,j}^{R} - P_{CL,0}\right) \times \left(t_{rs,(j+1)} - t_{rs,j}\right) \tag{14}$$

where, $P_{CL,j}^{R}$ = Critical active power available after restoration step j; j = Step index in critical load recovery, $t_{rs,j}$ = Restoration start time of j^{th} step.

3.3.3. Adapt

The system stability can be measured through its short circuit capacity (SCC), followed by voltage stability index (VSI), called adaptability index ($\Re_A$), expressed in (17). The incorporation of DERs is vital to increase the system resiliency; however, it affects the SCC of the distribution network. Moreover, the SCC is highly dependent on the voltage magnitudes of the distribution network buses. Thus, the SCC can be considered a VSI for the system, which represents the capacity of loads that can be served by the network. A larger value of SCC indicates that the network can have strong loading ability of a bus. Conversely, a small SCC indicates that the network is weak to support loads [33].

As a matter of resilience, the main aim is to serve more loads within the stability limit. Therefore, this index can show the system's stability before, during, and after the HILP event. The SCC, $S_{sc,j}$, is obtained by (15), followed by (16).

$$S^i_{sc,j} = E^i_{th,j} / Z^i_{th,j} \tag{15}$$

$$S^i_{sc,min,j} = 2S^i_{L,j}\left(1 + \sin \emptyset^i_j\right) / E^i_{th,j} \tag{16}$$

$$\Re_{A,j} = VSI_j = \frac{1}{N_{bus,j}} \sum_{i=1}^{N_{bus,j}} S^i_{sc,min,j} / S^i_{sc,j} \tag{17}$$

where $E^i_{th,j}$ and $Z^{ti}_{th,j}$ are Thevenin voltage and impedance of bus i at the j^{th} stage, respectively. N_{bus} is the number of network buses. $S^i_{L,j}$ and $\emptyset^i_j$ are the apparent power magnitude and power factor angle of bus i at the j^{th} stage, respectively. VSI_j is the VSI at the j^{th} stage. $S^i_{sc,j}$ and $S^i_{sc,min,j}$ are the SCC at the j^{th} stage and the minimal SCC, respectively. Note that the smaller VSI indicates better stability characteristics.

3.3.4. Prevent

Finally, the preventive measure can be considered from a few historical outages. Two parameters are crucial to prevent future power outages, failure rate, and outage duration; these parameters should be reduced. Thus, the system's robustness and responsiveness should be improved by MMG, reconfiguration, and mobile services. The consequence of power outages in terms of life threats, outage cost, and loss of load can be minimized. The preventive index is expressed in (18). The lower value of $\Re_P$ can signify that the system follows better resilient characteristics.

$$\Re_P = \sum_{i=1}^{N} \left(\Psi_i \times P_{lost\,i}\right) \tag{18}$$

where, Ψ_i = Total outage duration in i^{th} failure, $P_{lost,i}$ = Total power lost in i^{th} failure, N = Number of failures.

4. Case Study and Results

To assess the proposed resilience framework, the developed model is applied to the IEEE 33-bus ADS, which comprises four MGs, four TLs, and three MSUs. The total load of the test system is 3715 kW+ j2300 kVAR. Among 33 buses, 10 buses are considered CL-connected buses, as shown in Fig. 3. The MG includes the PV, DG, BES units, and load; the available capacity is presented in Table I. The power required for CL restoration is 1560 kW + j1285 kVAR. Furthermore, the critical bus data are shown in Table II. In the planning stage, four TLs are placed optimally as $B_8 - B_{21}$ (T_1), $B_9 - B_{15}$ (T_2), $B_{25} - B_{29}$ (T_3), and $B_{18} - B_{33}$ (T_4). Further, in the proposed

model, three MSUs are placed that can travel according to the restoration requirement. The placement is based on the optimization problem in (1). As can be seen from (1), denotes the MSU cost optimization formula, where C_h is the cost of fuel for moving between buses (as transportation cost) and $D_{h,t}$ is the distance traveled (taking 5 minutes to move from each bus to adjacent bus, which has been optimized by the SRSR optimization algorithm [34]). Further, it is assumed that the proper location of MSU can also reduce the recovery time and traveling cost. Therefore, three MSUs are used in three different zones, suchlike, $B_1\ to\ B_{11}$ – MSU1, $B_{12}\ to\ B_{22}$ – MSU2 and $B_{23} to\ B_{33}$ – MSU3 and the locations are assumed as B_{10}, B_{22}, and B_{23} for MSUs -1, 2, and 3, respectively. The reason for considering the three MSUs in three different zones is that it is assumed that in each zone, there should be a charging station to reduce the recovery time and traveling cost. The main aim of resilience is to restore the critical load as fast as possible, so recovery time should be faster, which minimizes the social and life threats.

Two different studies, such as single and multiple fault analyses, are conducted. Each study has three scenarios with different resource combinations, that is, without resources (WR) meaning only grid connected denoted as G is used, and then DERs, and reconfiguration (denoted as REC). In WR, only grid power is used to satisfy the load demand, and in DERs, PV, DG, and BES are used. Finally, in REC, TLs and MSUs in addition to DERs, are used to satisfy the CL demand.

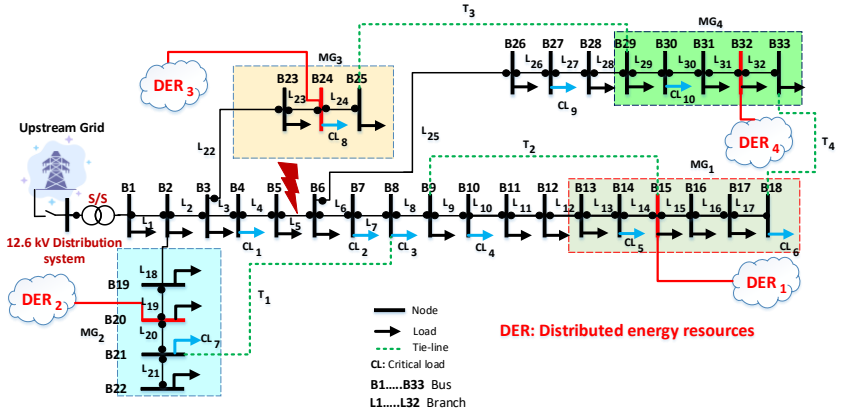

Fig. 3. IEEE 33-bus active distribution system with single fault

Table I. System data

MG	PV (MW)	BES (MW)	DG (MW)	MSU (MW)
1	0.5	0.4	0.2	
2	0.5	0.25	0.2	
3	1	0.5×2 = 1	0.25×2 = 0.5	0.25×3 = 0.75
4	1	0.35×2 = 0.7	0.2×2 = 0.4	

Table II. Critical load data

Bus	Bus data (kW +j kVAR)	MG	Bus	Bus data (kW + j kVAR)	MG
4	120 + j80	-	21	90 + j40	2
7	200 + j100	-	24	420 + j200	3
8	200 + j100	-	27	60+ j25	-
10	60+ j20	-	30	200 + j600	4
14	120 + j80	1	*Total*	*1560+ j1285*	
18	90 + j40	1			

4.1. Study-1: Single-fault scenario

If an extreme event occurs and line L_5 is out (as shown in Fig. 3), the restoration is performed according to different scenarios, discussed as follows.

4.1.1. Scenario-I: Disaster occurs at time 2 am (PV power = 0 and SOC = 0.9)

Although the grid is available after the event, it can only restore the critical loads CL_1, CL_7, and CL_8, but other CLs cannot be restored because the remaining system has an outage after L_5. However, with the installation of DERs and formation as MGs, they can switch to islanding mode when necessary. All the MGs are in islanding mode after the events, and the critical loads inside the MG can easily be restored. However, in this scenario, the PV is unavailable, and some CLs can be restored through BES, as presented in Table III. On the contrary, using REC, the grid supply can be fed directly to CLs through TLs to restore all the CLs. Tables IV and V present the participation of available resources and restoration paths, respectively.

4.1.2. Scenario-II: Disaster occurs at time 2 pm (PV power available at peak and SOC = 0.2)

In this scenario, the PV power and grid are available to restore the CL after the event. The WR case is the same as scenario I. In the DER case, all the MGs are switched to islanding mode, and the loads connected to MGs are restored. However, the CLs outside the MG, such as CL_2, CL_3, CL_4, and CL_9, cannot be restored. Although CL_1 is outside the MG, it can be restored due to the available grid power. Furthermore, using REC mode, the MG-connected CL is able to restore itself, and the grid power through TL restores CL outside the MG. Tables VI, VII, and VIII present the resource availability, participation of different resources, and restoration paths, respectively.

Table III. Available resources corresponding to CL recovery

	G	PV	BES	DG	CL recoverd	Open switch
WR	✓	×	×	×	CL_1, CL_7, CL_8	L_5
DERs	✓	×	✓	×	CL_1, CL_5, CL_6, CL_7, CL_8,CL_{10}	L_5, L_{12}, L_{28}
REC	✓	×	×	×	All	L_5, T_2, T_3, T_4

Table IV. Participation

	PV (MW)	DG (MW)	BES (MW)	MSU (MW)	Total load served (MW)	CL served (MW)
DERs	×	0.2	1.95	×	2.79	0.98
REC	×	0	0	×	3.715	1.56

Table V. Resources and restoration path for CL recovery

CL	G	MG	TL	MSU	Recovery Path
CL_1	✓	×	×	×	B_1- L_1- L_2 - L_3 - B_4
CL_2	✓	×	✓	×	B_1- L_1- L_{18} -L_{20} - T_1-L_7-B_7
CL_3	✓	×	✓	×	B_1- L_1- L_{18} - L_{20} - T_1 – B_8
CL_4	✓	×	✓	×	B_1- L_1- L_{18}- L_{20} -T_1-L_8 - L_9- B_{10}
CL_5	×	MG_1	×	×	B_{15} - L_{14} - B_{14}
CL_6	×	MG_1	×	×	B_{15} - L_{15} - L_{16} - L_{17}- B_{18}
CL_7	×	MG_2	×	×	B_{20} - L_{20} - B_{21}
CL_8	×	MG_3	×	×	B_{24}
CL_9	✓	×	×	×	B_1- L_1- L_{18} -L_{20} -T_1-L_7- L_6- L_{25}- L_{26}- B_{27}
CL_{10}	×	MG_4	×	×	B_{32} - L_{31} - L_{30} - B_{30}

4.1.3.Scenario-III: Disaster occurs at time 2 pm (PV power available at peak and SOC = 0.9)

This scenario is relatively similar to scenario II. If the grid and PV power are available, other resources are not required. The MG-connected CL can be restored by itself, and other CLs can be restored through grid power using TL. Tables IX, X, and XI present the detailed analysis of scenario III.

Remark: If the grid is less vulnerable and there is a single-fault event, the grid can supply the CL through TL. Moreover, the capacity of BES can sometimes be insufficient to satisfy the demand, and MGs can use the grid power to restore the load. If the grid power and PV generations are available, the stored power shouldn't be used but be kept for an emergency purpose. Thus, the MG's operation cost can be reduced. DGs can also be used when necessary. Usually, it is not preferred due to the high operating cost. Moreover, the MSU is not required to travel in such type of event as long as the CL can be restored through any combinations (grid, TL, BES, and PV). The final restored network is shown in Fig. 4.

Table VI. Available resources corresponding to CL recovery

	G	PV	BES	DG	CL recoverd	Open switch
WR	✓	×	×	×	CL_1, CL_7, CL_8	L_5
DERs	✓	✓	×	×	CL_1, CL_5, CL_6, CL_7, CL_8,CL_{10}	L_5, L_{12}, L_{28}
REC	✓	✓	×	×	All	L_5, L_{12}, L_{28}, T_2, T_3, T_4

Table VII. Participation

	PV (MW)	DG (MW)	BES (MW)	MSU (kW)	Total load served (MW)	CL served (MW)
DERs	2.6	×	×	×	2.79	1.04
REC	2.6	×	×	×	3.715	1.56

Table VIII. Resources and restoration path for CL recovery

CL	G	MG	TL	MSU	Recovery Path
CL_1	✓	×	×	×	B_1- L_1- L_2 - L_3 -B_4
CL_2	✓	×	✓	×	B_1- L_1- L_{18} - L_{20} - T_1-L_7- B_7
CL_3	✓	×	✓	×	B_1- L_1- L_{18} -L_{20} - T_1 - B_8
CL_4	✓	×	✓	×	B_1- L_1- L_{18} - L_{20} -T_1-L_8- L_9- B_{10}
CL_5	×	MG_1	×	×	B_{15} - L_{14} - B_{14}
CL_6	×	MG_1	×	×	B_{15} - L_{15} - L_{16} - L_{17}- B_{18}
CL_7	×	MG_2	×	×	B_{20} - L_{20} - B_{21}
CL_8	×	MG_3	×	×	B_{24}
CL_9	✓	×	×	×	B_1-L_1-L_{18}-L_{20}-T_1-L_7-L_6- L_{25}-L_{26}- B_{27}
CL_{10}	×	MG_4	×	×	B_{32} - L_{31} - L_{30} - B_{30}

Table IX. Available resources corresponding to CL recovery

	G	PV	BES	DG	CL recoverd	Open switch
WR	✓	×	×	×	CL_1, CL_7, CL_8	L_5
DERs	✓	✓	×	×	CL_1, CL_5, CL_6, CL_7, CL_8,CL_{10}	L_5, L_{12}, L_{28}
REC	✓	✓	×	×	All	L_5, L_{12}, L_{28}, T_2, T_3, T_4

Table X. Participation

	PV (MW)	DG (MW)	BES (MW)	MSU (MW)	Total load served (MW)	CL served (MW)
DERs	2.6	×	×	×	2.79	1.04
REC	2.6	×	×	×	3.715	1.56

Table XI. Resources and restoration path for CL recovery

CL	G	MG	TL	MSU	Recovery Path
CL_1	✓	×	×	×	B_1- L_1- L_2 - L_3 – B_4
CL_2	✓	×	✓	×	B_1- L_1- L_{18} -L_{19} -L_{20} -T_1-L_7- B_7
CL_3	✓	×	✓	×	B_1- L_1- L_{18} -L_{19} -L_{20} -T_1 -B_8
CL_4	✓	×	✓	×	B_1- L_1-L_{18}-L_{19}-L_{20}-T_1-L_8 - L_9 -B_{10}
CL_5	×	MG_1	×	×	B_{15} - L_{14} - B_{14}
CL_6	×	MG_1	×	×	B_{15} - L_{15} - L_{16} - L_{17}- B_{18}
CL_7	×	MG_2	×	×	B_{20} - L_{20} - B_{21}
CL_8	×	MG_3	×	×	B_{24}
CL_9	✓	×	×	×	B_1- L_1- L_{18} -L_{19} -L_{20} - T_1-L_7- L_6- L_{25}- L_{26}- B_{27}
CL_{10}	×	MG_4	×	×	B_{32} - L_{31} - L_{30} - B_{30}

4.2. Study 2: Multiple-fault scenario

If a high disruptive event occurs and three lines, such as L_1, L_5, and L_7, are out (shown in Fig. 5), the restoration can be performed according to different scenarios.

4.2.1.Scenario I: Disaster occurs at time 2 am (PV power = 0 and SOC = 0.9)

During multiple faults, the grid power to the network is zero because the fault occurs on L_1. Therefore, in the case of WR, the restored CL is zero. With the incorporation of DERs, the PV power is zero according to the scenario. However, using BES and DG, some critical loads are restored, *i.e.*, 0.92 MW. Furthermore, reconfiguration techniques are applied with four TLs placed optimally, as shown in Fig. 3, and the optimal placements of MSUs are at B_{10}, B_{22}, and B_{23}. The remaining critical loads (CL_1, CL_2, CL_3, CL_4, and CL_9) are restored through MG and MSU's. The MG_3 and MG_4 have increased the capacity through DG and restored critical loads, such as CL1 and CL_9, respectively. In addition, the MSUs are then moved to locations B_7, B_8, and B_{10}, for the restoration of CL_2, CL_3, and CL_4. For CL_2, MSU can travel from B_{23} to B_7 and then recover CL_2; for CL_3, other MSUs can travel from B_{22} to B_8 and recover CL_3; for CL_4, an MSU is in the same place as per the optimal location, can be seen in Fig. 6(a). Finally, the open switch location, participation, and recovery paths are presented in Tables XII, XIII, and XIV, respectively.

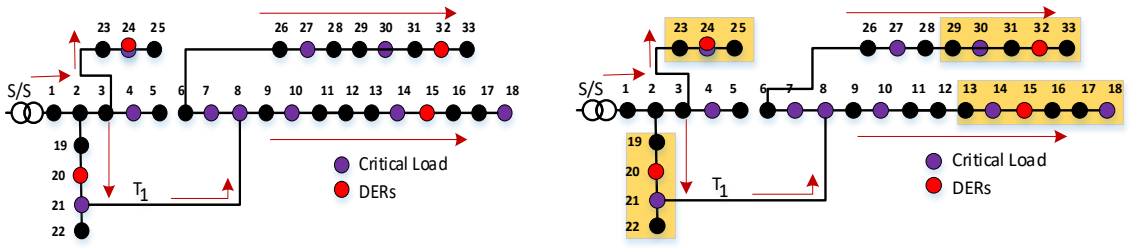

(a) (b)

Fig. 4. Final restored network: (a) Grid with TL, (b) Grid, MG, and TL

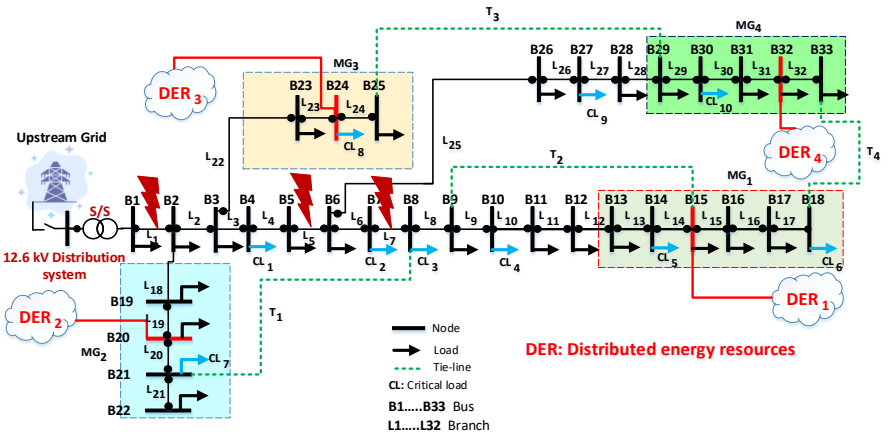

Fig. 5. IEEE 33-bus active distribution system with multiple faults

4.2.2. Scenario II: Disaster occurs at time 2 pm (PV power available at peak and SOC = 0.2)

As shown in Tables XV and XVI, considering WR, the entire system is blackout as the grid fails and no resources are used to restore the loads after the events. By using DERs and according to the scenario, the PV power is available, but SOC is 0.2. The critical load of 0.92 MW can be restored using PV and DG. Furthermore, in REC case, the capacity of MG_3 is increased through DG, and CL_1 is restored. Similarly, with increased capacity of MG_4, CL_9 can be restored. In addition, the MSU is then moved to the appropriate locations, such as B_{10}, for the restoration of CL_4. For CL_4, no travel is required because an MSU is in the same place as the optimal location. For CL_2, the MSU at bus B_{22} can travel to B_7. CL_3 can be restored through T_1 using MG_2. The final restored network can be seen in Fig. 6(b), and Table XVI shows the responsible resources and path for the restoration.

Table XII. Available resources corresponding to CL recovery

	PV	BES	DG	MSU	CL recoverd	Open switch
WR	×	×	×	×	-	L_1, L_5, L_7
DERs	×	✓	✓	×	CL_5, CL_6, CL_7, CL_8, CL_{10}	L_1, L_5, L_7, L_{12}, L_{28}
REC	×	✓	✓	✓	All	L_1, L_5, L_7, L_8, L_9, L_{10}, L_{12},T_1, T_2, T_3, T_4

Table XIII. Participation

	PV (MW)	DG (MW)	BES (MW)	MSU (MW)	Total load served (MW)	CL served (MW)
DERs	×	0.85	1.95	×	2.48	0.92
REC	×	1.3	1.95	0.75	3.175	1.56

Table XIV. Resources and restoration path for CL recovery

CL	MG	TL	MSU	Recovery path
CL_1	MG_3	×	×	B_{24}- L_{23}- L_{22} - L_3-B_4
CL_2	×	×	✓	MSU_2 - B_7
CL_3	×	×	✓	MSU_3- B_8
CL_4	×	×	✓	MSU_1 - B_{10}
CL_5	MG_1	×	×	B_{15} - L_{14} - B_{14}
CL_6	MG_1	×	×	B_{15} - L_{15} - L_{16} - L_{17}- B_{18}

CL_7	MG_2	×	×	B_{20} - L_{20} -B_{21}
CL_8	MG_3	×	×	B_{24}
CL_9	MG_4	×	×	B_{32} - L_{31} ….- L_{27} - B_{27}
CL_{10}	MG_4	×	×	B_{32} - L_{31} - L_{30} - B_{30}

4.2.3.Scenario III: Disaster occurs at time 2 pm (PV power available at peak and SOC = 0.9)

As reported in Tables XVII and XIX, considering WR, the entire system is blackout as the grid fails and no resources are used to restore the loads after the events. In DERs case, according to the scenario, the PV power is available, and SOC is 0.9. The critical load of 920 kW can be restored using PV and BES units. Furthermore, through REC technique, the MG capacities are increased through BES, and restoration operation is performed, as shown in Table XX, and the restored network is shown in Fig. 6(c).

Table XV. Available resources corresponding to CL recovery

	G	PV	BES	DG	MSU	CL recovered	Open switch
WR	×	×	×	×	×	-	L_1, L_5, L_7
DERs	×	✓	×	✓	×	CL_5, CL_6, CL_7, CL_8, CL_{10}	L_1, L_5, L_7, L_{12}, L_{28}
REC	×	✓	×	✓	✓	All	L_1, L_2, L_5, L_7, L_8, L_9, L_{10}, L_{12}, T_2, T_3, T_4

Table XVI. Participation

	PV (MW)	DG (MW)	BES (MW)	MSU (MW)	Total load served (MW)	CL served (MW)
DERs	2.4	0.45	0	×	2.48	0.92
REC	2.4	0.85	0	0.5	3.36	1.56

Table XVII. Resources and restoration path for CL recovery

CL	MG	TL	MSU	Recovery path
CL_1	MG_3	×	×	B_{24}- L_{23}- L_{22} - L_3 - B_4
CL_2	-	×	✓	MSU_2 - B_7
CL_3	MG_2	T_1	×	B_{20}- L_{20} - T_1 – B_8
CL_4	MG_1	×	✓	MSU_1 - B_{10}
CL_5	MG_1	×	×	B_{15} - L_{14} - B_{14}
CL_6	MG_1	×	×	B_{15} - L_{15} - L_{16} - L_{17} - B_{18}
CL_7	MG_2	×	×	B_{20} - L_{20} - B_{21}
CL_8	MG_3	×	×	B_{24}
CL_9	MG_4	×	×	B_{32} - L_{31} ….- L_{27} - B_{27}
CL_{10}	MG_4	×	×	B_{32} - L_{31} - L_{30}- B_{30}

Table XVII. Available resources corresponding to CL recovery

	PV	BES	DG	MSU	CL recovered	Open switch
WR	×	×	×	×	-	L_1, L_5, L_7
DERs	✓	✓	×	×	CL_5, CL_6, CL_7, CL_8, CL_{10}	L_1, L_5, L_7, L_{12}, L_{28}

REC	✓	✓	×	×	All	L_1, L_2, L_5, L_7, L_8, L_{10}, L_{12},T_3, T_4

TABLE XIX. Participation

	PV (MW)	DG (MW)	BES (MW)	MSU (MW)	Total load served (MW)	CL served (MW)
DERs	2.4	×	0.7	×	2.48	0.92
REC	2.4	×	1.4	×	3.55	1.56

Table XX. Resources and restoration path for CL recovery

CL	MG	TL	MSU	Recovery path
CL_1	MG_3	×	×	B_{24}- L_{23}- L_{22} - L_3 - B_4
CL_2	MG_4	×	×	B_{32} - L_{31} .... L_{25} - L_6- B_7
CL_3	MG_3	T_1	×	B_{20}- L_{20} - T_1 - B_8
CL_4	MG_1	T_2	×	B_{15} - T_2 - B_9- B_{10}
CL_5	MG_1	×	×	B_{15} - L_{14}- B_{14}
CL_6	MG_1	×	×	B_{15} - L_{15} - L_{16} - L_{17}- B_{18}
CL_7	MG_2	×	×	B_{20} - L_{20} -B_{21}
CL_8	MG_3	×	×	B_{24}
CL_9	MG_4	×	×	B_{32} - L_{31} ….- L_{27}- B_{27}
CL_{10}	MG_4	×	×	B_{32} - L_{31} - L_{30}- B_{30}

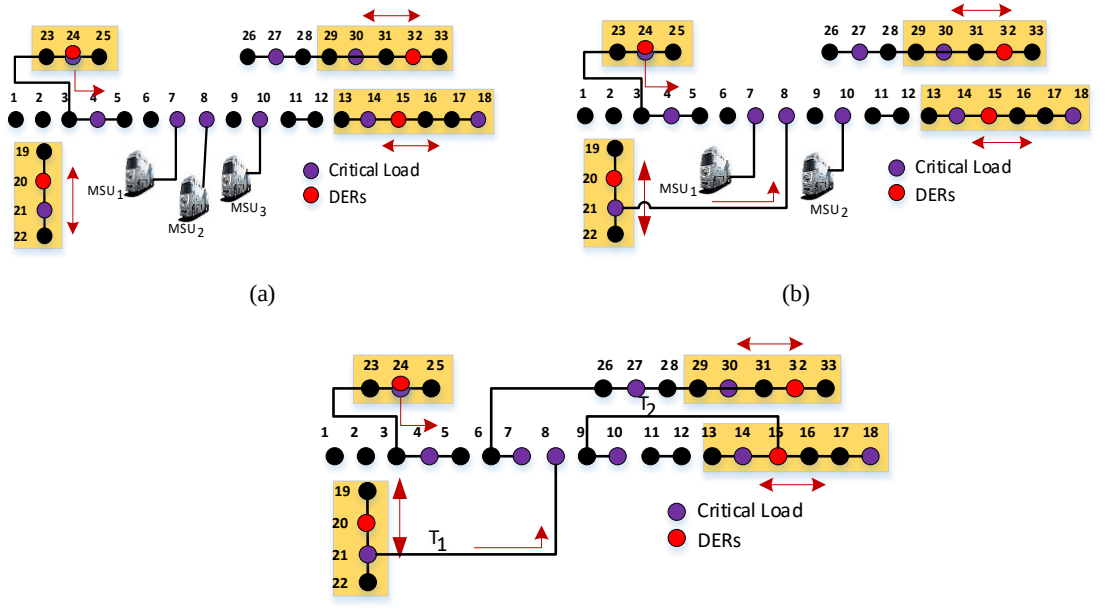

(a) (b)

(c)

Fig. 6. Final restored network corresponding to (a) Scenario I, (b) Scenario II, (c) Scenario III

Remark: During the event of multiple faults, DG's and MSU's participation are vital for restoration. The emergency resources are integrated because DGs are highly expensive, and the recovery time becomes longer using MSUs because the grid supply fails and the load point cannot be reached through TL. However, life threats and critical services should be considered. On that premise, resourcefulness is extremely important during multiple event scenarios. All the CLs can be restored using reconfiguration techniques. On the contrary, as reported in

Tables XII, XV, and XVII, more open switches are needed in multiple fault scenarios than a single fault. Thus, line switching is also important to manage priority-based restoration.

4.3. Performance comparison with resilience index

In this section, four resilience indices are evaluated, corresponding to three scenarios. Each index has its own significance as reported in a tabular form along with the improvement. During the event, the contribution of DERs is pivotal because the grid might fail to supply the CLs. Thus, the CLs should be restored as quickly as possible. Table XXI shows the $\Re_W$ value, which indicates that the CL is available after the event. According to scenarios I, II, and III, the availability of resources can withstand the system in the wake of extreme events. Further, the increased coping capacity is shown in Table XXI, where the reference value is taken as 0.63 MW. The reference value is taken here as 0.63 MW due to the following reasons.

In a single fault system, the fault happens on line L_5. In this case, the resulting grid does not have tie-line and MG connections. The grid can recieve power from the nodes as: B_1 to B_5, B_2 to B_{22}, and B_3 to B_{25}, where only three critical loads are available (see Fig. 5) such as B_4 (120 kW), B_{21} (90kW), and B_{24} (420kW). The total sum is 120+90+420 = 630 kW (= 0.63 MW). After the MG connection, the load has been increased to 0.98 (0.63+0.35) MW, then after adding the tie-line, the load is 0.63+0.41=1.04 MW (see Table-XXI) using WR, and this is the available CL value after the events. Accordingly, the values are increased using different resource combinations. It is noted that scenarios II and III have the same value because the PV power is available in both cases; thus, sufficient energy can restore the CL as per the feasibility. In this case, TL and MSU are not considered. The grid is unavailable under multiple faults; thus, with DERs, the system can restore the maximum loads inside the MGs.

Table XXI. Withstand capacity and its improvement

	Scenario	$\Re_W$ (MWh)	Coping capacity Increased (MW)
Study-1: Single fault	I	0.35	0.98
	II	0.41	1.04
	III	0.41	1.04
Study-2: Multiple faults	I	0.83	0.83
	II	0.92	0.92
	III	0.92	0.92

Recovery phase starts from t_{rs}. In an initial attempt, the grid and MGs can restore the CLs. However, these resources cannot restore all the CLs, and then TLs are used with grid and MGs. During the single-fault case, MSUs are not required because, through TL, all CLs can be restored, as shown in Table XXII. On the contrary, during the multiple faults, the reconfiguration of the system is crucial, and MSUs are used, as reported in Table XXII. Moreover, the restoration is improved using a combination of resources. In Scenario III, MSUs do not participate because the available PV power and BES can restore all the CLs through TL. As far as adaptability is concerned, the system should be stable irrespective of the event's occurrence in the network. On the other hand, the voltage should be in the limiting range to avoid system collapse. Thus, the voltage stability index is measured in this study, presented in Table XXIII, corresponding to various scenarios. Table XXIII presents the VSI using different

resource combinations. It can be seen that in the event of a single fault, the VSI is better than the multiple fault for each scenario. Notably, with grid supply, the system can follow the better stability characteristics; without grid supply, the system would utilize the DERs which are intermittent in nature, and accordingly, the stability of the system decreases. The utilization of both PV and storage (in scenario-III) has considerably enhanced the stability performance as compared to scenario-I (storage only) and scenario-II (PV only) in the context of VSI in both of the single-fault and multi-fault cases. To prevent future power outages, the previous experience and outage data are greatly important.

Table XXII. Recovery and its improvement

	Scenario	Resource	$\Re_R$(MWh)	CL Restoration Improvement (MW)
Study-1: Single fault	I	G+MG	0.01603	0.98
		G+MG+TL	0.03348	1.56
	II	G+MG	0.017056	1.04
		G+MG+TL	0.06417	1.56
	III	G+MG	0.017056	1.04
		G+MG+TL	0.06417	1.56
Study-2: Multiple faults	I	G+MG	0.0382	0.92
		G+MG+TL	0.069	1.38
		G+MG+TL+MSU	3.96	1.56
	II	G+MG	0.05038	1.1
		G+MG+TL	0.06318	1.30
		G+MG+TL+MSU	3.30	1.56
	III	G+MG	0.0115	0.92
		G+MG+TL	0.02896	1.56

Table XXIII. Voltage stability index

Scenarios	$\Re_A$ (pu)	
	Single fault	Multiple faults
I	0.7459	0.9743
II	0.6589	0.6820
III	0.5347	0.6628

Table XXIV. Prevent index and its improvement

	Scenario	Resource	$\Re_P$(MWh)	Reduced impact
Study-1: Single fault	I	WR	1.86	-
		G+MG+TL	0.6	67.75 %
	II	WR	1.86	-
		G+MG+TL	0.522	71.94 %
	III	WR	1.86	-
		G+MG+TL	0.522	71.94 %
Study-2: Multiple faults	I	WR	9.36	-
		G+MG+TL	0.66	93.58%
		G+MG+TL+MSU	0.189	97.98 %
	II	WR	9.36	-

		G+MG+TL	0.4810	94.86 %
		G+MG+TL+MSU	0.2764	97.04 %
	III	WR	9.36	-
		G+MG+TL	0.647	93.08 %
		G+MG+TL+MSU	-	-

The system operator should analyze the outage data to prepare for future events. The impact of the power outage mainly depends on the number of failures and outage duration. To minimize the failure rate, the system should be hardened, that is, a decentralized network and better prediction strategy should be formed. On the other hand, to reduce the outage duration, the recovery should be faster, and this condition is possible through system reconfiguration using TLs and DERs, and the adaptive formation of MGs and mobile services, such as MSU, mobile substation, crews, and mobile de-icing devices. In the proposed system, the outages duration is minimized using the different resources. The minimization of the failure rate is out of the scope of this paper. In this case, the line repair takes 2 hours for each traditional system after the event ends, and after the reconfiguration, the system follows the exact recovery time from simulation. TABLE XXIV shows the prevent index and reduced impact in percentage.

The measured data of the preventive index represents a single-failure event in 24 hours. However, to verify the importance of the prevent index, N and Ψ should be changed. Thus, historical outage data are obtained from [35], representing the California power outage data. The state of California has one of the topmost frequent power outages in the US states. In 2020, the number of major power outage across California was 11, as shown in TABLE XXV. The evaluation of $\Re_P$ with different N and Ψ is discussed as follows. TABLES XXVI and XXVII present the prevent index with constant and reduced failure rates, respectively. Total duration of power outages in 2020 (Ψ) = 202.05 hrs, Total loss of power due to outages in 2020 = 7706 MW, Total number of failures (N) = 11. From (18), $\Re_{Pi} = 219189.3$ MWh

Table XXVI presents the preventive index for constant failure rate (N =11) and different Ψ. The outage duration is reduced (assume recovery is faster). Furthermore, considering the reduced failure rate, the prevent index is reduced, as shown in Table XXVII.

Table XXV. Major power outage in 2020 [35]

Sl No.	Event Date	Duration (hours)	Loss (MW)	Affected customer
1	01/17/2020	4.75	87	67864
2	02/17/2020	8.08	91	70000
3	03/16/2020	69	165	110800
4	08/14/2020	27.75	1680	> 500000
5	08/16/2020	34.56	1580	> 500000
6	08/18/2020	7	917	>200000
7	09/05/2020	3.28	986	> 200000
8	09/7/2020	42.73	610	172000
9	09/27/2020	20.83	337	102267
10	10/25/2020	51.46	1218	370000

11	12/17/2020	0.416	35	170000
	Total	202.05	7706	

Table XXVI Constant failure rate (N=11)

Ψ (hours) (Reduced by)	$\Re_P$(MWh)
1/4	109594.6
1/3	73063.1
1/2	54797.3

Table XXVII. Reduced failure rate

N	$\Re_P$(MWh)
9	156496.4
6	120177.3
3	12533.5

As far as the reduced preventive index is concerned, it directly impacts the outage cost. According to the US Department of Energy, the outages cost an average of about $18 billion to $53 billion per year in the US [36]. So, boosting the power system resiliency is essential.

5. Conclusion

This paper presents the novel resilience quantification framework WRAP to design a resilient ADS in the wake of extreme events. With the WRAP framework, the coping capacity, fast recovery, system stability, and preventive measure are quantified during and after the event, and the enhancement of these indices is also discussed. Moreover, the system resiliency is measured when the available resources are utilized optimally. Furthermore, MSU is added, and its participation is vital for critical load restoration in multiple fault scenarios. The result of the applied test system has proven that resourcefulness is the prior requirement in the context of resilience; it can minimize the catastrophic consequences in an extreme unfolding event. This study is limited to a single renewable source, such as PV systems. However, in future research, the integration of more renewable, ancillary devices, and hardening plans can be considered to enhance the robustness and fast recovery of the system. Furthermore, better prediction techniques using machine learning can be applied to minimize future attacks for preventive measures. The proposed framework can provide a better planning and operation scheme, which can be applied to the standard test system to quantify the resilience characteristics and compare them with existing studies.

6. Reference

[1] Y. Wang, C. Chen, J. Wang, and R. Baldick, "Research on resilience of power systems under natural disasters—A review," *IEEE Transactions on Power Systems,* vol. 31, no. 2, pp. 1604-1613, 2015.

[2] M. Panteli and P. Mancarella, "The grid: Stronger, bigger, smarter?: Presenting a conceptual framework of power system resilience," *IEEE Power and Energy Magazine,* vol. 13, no. 3, pp. 58-66, 2015.

[3] L. Che, M. Khodayar, and M. Shahidehpour, "Only connect: Microgrids for distribution system restoration," *IEEE power and energy magazine,* vol. 12, no. 1, pp. 70-81, 2013.

[4] Z. Bie, Y. Lin, G. Li, and F. Li, "Battling the extreme: A study on the power system resilience," *Proceedings of the IEEE,* vol. 105, no. 7, pp. 1253-1266, 2017.

[5] D. K. Mishra, M. J. Ghadi, L. Li, and J. Zhang, "Proposing a Framework for Resilient Active Distribution Systems using Withstand, Respond, Adapt, and Prevent Element," in *2019 29th Australasian Universities Power Engineering Conference (AUPEC)*, 2019, pp. 1-6: IEEE.

[6] M. H. Amirioun, F. Aminifar, and M. Shahidehpour, "Resilience-promoting proactive scheduling against hurricanes in multiple energy carrier microgrids," *IEEE Transactions on Power Systems,* vol. 34, no. 3, pp. 2160-2168, 2018.

[7] L. Che and M. Shahidehpour, "Adaptive formation of microgrids with mobile emergency resources for critical service restoration in extreme conditions," *IEEE Transactions on Power Systems,* vol. 34, no. 1, pp. 742-753, 2018.

[8] M. Nazemi, M. Moeini-Aghtaie, M. Fotuhi-Firuzabad, and P. Dehghanian, "Energy storage planning for enhanced resilience of power distribution networks against earthquakes," *IEEE Transactions on Sustainable Energy,* vol. 11, no. 2, pp. 795-806, 2019.

[9] S. Yao, P. Wang, X. Liu, H. Zhang, and T. Zhao, "Rolling optimization of mobile energy storage fleets for resilient service restoration," *IEEE Transactions on Smart Grid,* vol. 11, no. 2, pp. 1030-1043, 2019.

[10] Y. Liu, Y. Li, H. Xin, H. B. Gooi, and J. Pan, "Distributed optimal tie-line power flow control for multiple interconnected AC microgrids," *IEEE Transactions on Power Systems,* vol. 34, no. 3, pp. 1869-1880, 2018.

[11] S. Lei, C. Chen, Y. Li, and Y. Hou, "Resilient disaster recovery logistics of distribution systems: Co-optimize service restoration with repair crew and mobile power source dispatch," *IEEE Transactions on Smart Grid,* vol. 10, no. 6, pp. 6187-6202, 2019.

[12] T. Ding, Z. Wang, W. Jia, B. Chen, C. Chen, and M. Shahidehpour, "Multiperiod Distribution System Restoration with Routing Repair Crews, Mobile Electric Vehicles, and Soft-Open-Point Networked Microgrids," *IEEE Transactions on Smart Grid,* 2020.

[13] S. Abbasi, M. Barati, and G. J. Lim, "A parallel sectionalized restoration scheme for resilient smart grid systems," *IEEE Transactions on Smart Grid,* vol. 10, no. 2, pp. 1660-1670, 2017.

[14] P. Bajpai, S. Chanda, and A. K. Srivastava, "A novel metric to quantify and enable resilient distribution system using graph theory and choquet integral," *IEEE Transactions on Smart Grid,* vol. 9, no. 4, pp. 2918-2929, 2016.

[15] G. Huang, J. Wang, C. Chen, J. Qi, and C. Guo, "Integration of preventive and emergency responses for power grid resilience enhancement," *IEEE Transactions on Power Systems,* vol. 32, no. 6, pp. 4451-4463, 2017.

[16] N. L. Dehghani, Y. M. Darestani, and A. Shafieezadeh, "Optimal life-cycle resilience enhancement of aging power distribution systems: A MINLP-based preventive maintenance planning," *IEEE Access,* vol. 8, pp. 22324-22334, 2020.

[17] H. H. Abdeltawab and Y. A.-R. I. Mohamed, "Mobile energy storage scheduling and operation in active distribution systems," *IEEE Transactions on Industrial Electronics,* vol. 64, no. 9, pp. 6828-6840, 2017.

[18] S. Yao, P. Wang, and T. Zhao, "Transportable energy storage for more resilient distribution systems with multiple microgrids," *IEEE Transactions on Smart Grid,* vol. 10, no. 3, pp. 3331-3341, 2018.

[19] S. Lei, C. Chen, H. Zhou, and Y. Hou, "Routing and scheduling of mobile power sources for distribution system resilience enhancement," *IEEE Transactions on Smart Grid,* vol. 10, no. 5, pp. 5650-5662, 2018.

[20] M. Panteli, P. Mancarella, D. N. Trakas, E. Kyriakides, and N. D. Hatziargyriou, "Metrics and quantification of operational and infrastructure resilience in power systems," *IEEE Transactions on Power Systems,* vol. 32, no. 6, pp. 4732-4742, 2017.

[21] M. Amirioun, F. Aminifar, H. Lesani, and M. Shahidehpour, "Metrics and quantitative framework for assessing microgrid resilience against windstorms," *International Journal of Electrical Power & Energy Systems,* vol. 104, pp. 716-723, 2019.

[22] M. Panteli, C. Pickering, S. Wilkinson, R. Dawson, and P. Mancarella, "Power system resilience to extreme weather: fragility modeling, probabilistic impact assessment, and adaptation measures," *IEEE Transactions on Power Systems,* vol. 32, no. 5, pp. 3747-3757, 2016.

[23] H. Farzin, M. Fotuhi-Firuzabad, and M. Moeini-Aghtaie, "Enhancing power system resilience through hierarchical outage management in multi-microgrids," *IEEE Transactions on Smart Grid,* vol. 7, no. 6, pp. 2869-2879, 2016.

[24] X. Liu, M. Shahidehpour, Z. Li, X. Liu, Y. Cao, and Z. Bie, "Microgrids for enhancing the power grid resilience in extreme conditions," *IEEE Transactions on Smart Grid,* vol. 8, no. 2, pp. 589-597, 2016.

[25] J. Najafi, A. Peiravi, and J. M. Guerrero, "Power distribution system improvement planning under hurricanes based on a new resilience index," *Sustainable cities and society,* vol. 39, pp. 592-604, 2018.

[26] C. Shao, M. Shahidehpour, X. Wang, X. Wang, and B. Wang, "Integrated planning of electricity and natural gas transportation systems for enhancing the power grid resilience," *IEEE Transactions on Power Systems,* vol. 32, no. 6, pp. 4418-4429, 2017.

[27] D. N. Trakas, M. Panteli, N. D. Hatziargyriou, and P. Mancarella, "Spatial risk analysis of power systems resilience during extreme events," *Risk Analysis,* vol. 39, no. 1, pp. 195-211, 2019.

[28] Z. Li, M. Shahidehpour, F. Aminifar, A. Alabdulwahab, and Y. Al-Turki, "Networked microgrids for enhancing the power system resilience," *Proceedings of the IEEE,* vol. 105, no. 7, pp. 1289-1310, 2017.

[29] P. Jamborsalamati, M. Hossain, S. Taghizadeh, G. Konstantinou, M. Manbachi, and P. Dehghanian, "Enhancing power grid resilience through an IEC61850-based ev-assisted load restoration," *IEEE Transactions on Industrial Informatics,* vol. 16, no. 3, pp. 1799-1810, 2019.

[30] D. K. Mishra, P. K. Ray, L. Li, J. Zhang, M. Hossain, and A. Mohanty, "Resilient control based frequency regulation scheme of isolated microgrids considering cyber attack and parameter uncertainties," *Applied Energy,* vol. 306, p. 118054, 2022.

[31] V. Venkataramanan, A. Hahn, and A. Srivastava, "CP-SAM: Cyber-physical security assessment metric for monitoring microgrid resiliency," *IEEE Transactions on Smart Grid,* vol. 11, no. 2, pp. 1055-1065, 2019.

[32] V. Venkataramanan, A. K. Srivastava, A. Hahn, and S. Zonouz, "Measuring and enhancing microgrid resiliency against cyber threats," *IEEE Transactions on Industry Applications,* vol. 55, no. 6, pp. 6303-6312, 2019.

[33] A. Azizivahed, H. Narimani, E. Naderi, M. Fathi, and M. R. Narimani, "A hybrid evolutionary algorithm for secure multi-objective distribution feeder reconfiguration," *Energy,* vol. 138, pp. 355-373, 2017.

[34] M. Bakhshipour, M. J. Ghadi, and F. Namdari, "Swarm robotics search & rescue: A novel artificial intelligence-inspired optimization approach," *Applied Soft Computing,* vol. 57, pp. 708-726, 2017.

[35] Major Disturbances and Unusual Occurrences, Year-to-Date 2020 [Online]. Available: https://www.eia.gov/electricity/monthly/epm_table_grapher.php?t=epmt_b_1

[36] S. A. Shield, S. M. Quiring, J. V. Pino, and K. Buckstaff, "Major impacts of weather events on the electrical power delivery system in the United States," *Energy,* vol. 218, p. 119434, 2021.